Fiber-pigtailed silicon photonic sensors for methane leak detection

Chu C. Teng[1], Chi Xiong[2], Eric J. Zhang[2], Yves Martin[2], Marwan Khater[2], Jason Orcutt[2], William M. J. Green[2], and Gerard Wysocki[1]

[1]Department of Electrical Engineering, Princeton University, Princeton, NJ 08540
[2]IBM Thomas J. Watson Research Center, 1101 Kitchawan Rd, Yorktown Heights, NY 10598
ccteng@princeton.edu

Abstract: We present comprehensive characterization of silicon photonic sensors for methane leak detection. Sensitivity of 40 ppmv after 1 second integration is reported. Fourier domain characterization of on-chip etalon drifts is used for further sensor improvement.

OCIS codes: (300.0300) Spectroscopy; (280.4788) Optical sensing and sensors; (230.3120) Integrated optics devices; (280.1120) Air pollution monitoring.

1. Introduction

Cost-effective, sensitive, and accurate methane monitoring is critical for the reduction of methane leakage from natural gas production [1]. Integrated silicon photonic (SiPh) chip sensors have been demonstrated for evanescent field spectroscopy of CH_4 near λ = 1651 nm [2, 3], showing the feasibility of this on-chip sensor for such applications. As a result of refined design and fabrication of on-chip silicon waveguides, and robust mechanical stability gained from fiber-pigtailed assemblies, a nearly 20x improvement of the detection limit previously quoted in [1] is presented in this paper. As the sensor is currently limited by etalon fringe drift, we characterize the etalon free spectral range and their drifts under controlled thermal tuning of the SiPh chip.

2. Fiber-pigtailed silicon photonic chip sensor

Figure 1(a) shows a fiber-pigtailed SiPh chip that features a dual 10 cm-long spiral waveguide design with a 50/50 directional coupler, allowing for simultaneous measurements of two neighboring waveguides via the coupler's drop and thru ports. Three high numerical aperture optical fibers residing in glass v-groove sub-assemblies are actively aligned and attached to the polished facets of the SiPh chip with an index-matched optical adhesive. The chip and v-grooves are then mounted to a glass substrate for strain relief. As the Allan stability analysis of two such fiber-pigtailed prototypes in Fig. 1 (b) shows, the evanescent waveguide sensor can reach a detection limit between 40-50 ppmv with 1 second integration time. The improvement in sensitivity shown here as compared to the sensor characterized in [2] is a result of the mechanically stable chip-fiber coupling via the fiber-pigtailed assembly, as well as the reduced waveguide propagation loss and thus increased signal to noise ratio at the optical receiver output.

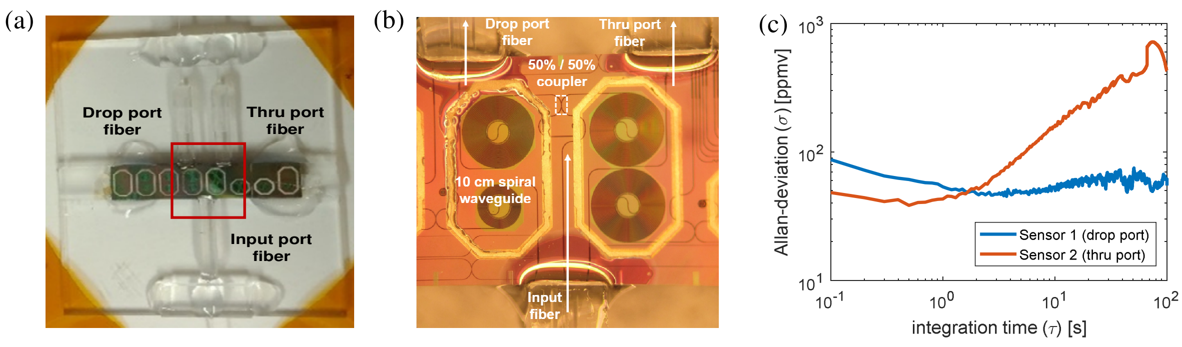

Figure 1: (a) Fiber-pigtailed silicon photonic sensor prototype. Both the drop port and thru port spiral waveguides are exposed to air, each having 10 cm-long optical paths. (b) Microscope image of the spiral waveguides located in the boxed region in (a). (c) Zero-gas Allan deviation analysis comparing two different fiber-pigtailed prototypes. A detection limit of 40-50 ppmv with 1 second integration time is obtained. Note that the detection limit calculation uses an experimentally verified effective modal overlap of 25% when operating with TM polarization.

The slightly better performance of Sensor 2 in the short term (< 1s) is attributable to lower fiber-waveguide coupling loss, resulting in larger relative optical power incident on the output photodetector. One goal for the next generation chip package is therefore to improve optical throughput, to prevent detector noise limited performance in the short term.

3. Thermal characterization of on-chip etalons

Since the on-chip waveguides are prone to parasitic reflections [4], Fig. 1 (b) also shows that current sensor performance is limited by fringe drift starting as early as 1 second. While further suppression of the etalon amplitudes is an ongoing objective in sensor fabrication (through design of low-reflectivity fiber-waveguide couplers and effective line edge roughness reduction), it is important to identify the origin and understand the behavior of these etalons in order to target our efforts towards etalon mitigation.

Through thermal tuning of the sensor chip via a thermoelectrically cooled stage, we induce etalon drifts that are visible from the zero gas spectra shown in Fig. 2(a). The Fourier transform of the ~210 second-long zero gas spectral dataset is used to quantify the etalon free spectral ranges (FSRs) and their relative amplitudes and phases. The magnitude of the Fourier transform is shown in Fig. 2(b), where we note three main cavities present along the tested waveguide. These etalons correspond to cavity lengths of ~ 0.6 cm, 5.1 cm, and 10.0 cm, assuming a calculated optical group index of 3.9. Indeed, we identified lithographic defects located at the center of the spirals that can explain the 5.1 cm long cavities, whereas the 10.0 cm cavity corresponds exactly to the waveguide length.

In addition, the movements of the etalons over time can be extracted from the phase of the Fourier transform. Fig. 2(c) shows the etalon shift of the three main cavities identified earlier. During the first ~80 seconds, we observe oscillations in etalon positions due to temperature instability at the beginning of the tuning process; the cold plate temperature is also shown in Fig. 2(c) for reference. As the temperature tuning rate becomes a constant 0.002 ºC/s, the etalons move linearly as is evident in both in Fig. 2(a) and more explicitly in Fig. 2(c). It is important to note that while the etalons from the two longer cavities (5.1 cm and 10.0 cm) move in sync (see Fig. 2(c)), the shortest cavity etalon moves at a slower rate for the same temperature tuning, suggesting a different thermo-optic coefficient from the other cavities. While these results prove that the movements of these etalons are directly related to thermal tuning of the chip, further study is underway to characterize their correlation with respect to each other.

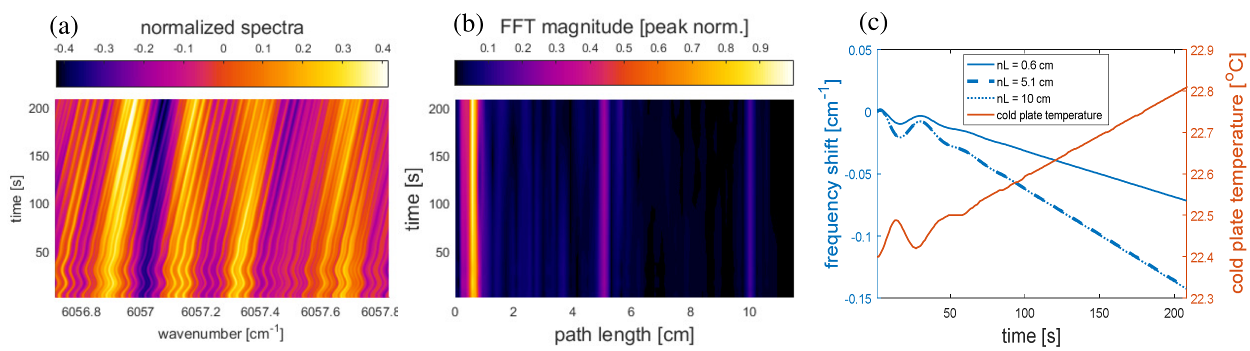

Figure 2: (a) Normalized (and mean subtracted) zero gas spectra as chip temperature is linearly tuned at a rate of 0.002 ºC/s; the waveguide sensor is operating in TE polarization. (b) Magnitude of Fourier transformed zero gas spectra in (a). (c) Extracted etalon shift of three prominent etalon features in units of wavenumber. Cold plate temperature measured during thermal tuning is also shown.

4. Conclusion

We have demonstrated a fiber-pigtailed silicon photonic chip sensor with ~40 ppmv sensitivity after 1 second of integration time, after which the system becomes limited by etalon drifts. On-chip etalons are characterized using the Fourier transform of zero gas spectra measured under temperature tuning of the sensor chip, and the analysis allows for convenient identification of etalon FSRs and the extraction of etalon frequency tuning. A unique feature of SiPh chip sensors is the compactness of waveguide layout, which leads to relatively uniform temperature fluctuations on-chip hence correlated etalon movements. Characterization of the various on-chip etalons is therefore a constructive step towards leveraging this correlation for fringe mitigation.

Acknowledgements: The information, data, or work presented herein was funded in part by the Advanced Research Projects Agency-Energy (ARPA-E), U.S. Department of Energy, under Award Number DE-AR0000540. The views and opinions of authors expressed herein do not necessarily state or reflect those of the United States Government or any agency thereof. The authors also recognize the IBM Microelectronics Research Laboratory for assistance with sensor fabrication.

5. References

[1] A. R. Brandt, et al. "Methane leaks from North American natural gas systems," Science, 343(6172), 733-735, (2014).

[2] Eric J. Zhang, et al, "Silicon photonic on-chip trace gas spectroscopy of methane," In Conference on Lasers and Electro-optics, San Jose, C.A., June 2016, pp. 2065-2069.

[3] William M. J. Green, et al, "Silicon photonics for on-chip trace-gas spectroscopy," Proceedings of the 3rd ACM International Conference on Nanoscale Computing and Communications, New York, N.Y., September 2016, pp. 21:1—21:2.

[4] Y. Xing, A. Li, R. Van Laer, R. Baets, W. Bogaerts, "Backscattering induced transmission noise and length dependent attenuation in silicon waveguides", 2016 IEEE Photonics Scociety Benelux Annual Symposium, Belgium, (2016)